Title	High speed photoacoustic tomography system with low cost portable pulsed diode laser
Author(s)	Upputuri, Paul Kumar; Sivasubramanian, Kathyayini; Pramanik, Manojit
Citation	Upputuri, P. K., Sivasubramanian, K., & Pramanik, M. (2015). High speed photoacoustic tomography system with low cost portable pulsed diode laser. Proceedings SPIE 9524,95240G.
Date	2015
URL	http://hdl.handle.net/10220/38387
Rights	© 2015 [SPIE] This paper was published in [Proceedings SPIE 9524] and is made available as an electronic reprint (preprint) with permission of [SPIE]. The published version is available at: [http://dx.doi.org/10.1117/12.2186136]. One print or electronic copy may be made for personal use only. Systematic or multiple reproduction, distribution to multiple locations via electronic or other means, duplication of any material in this paper for a fee or for commercial purposes, or modification of the content of the paper is prohibited and is subject to penalties under law.

High speed photoacoustic tomography system with low cost portable pulsed diode laser

Paul Kumar Upputuri, Kathyayini Sivasubramanian, and Manojit Pramanik[a]
School of Chemical and Biomedical Engineering, Nanyang Technological University, Singapore 637459

ABSTRACT

Photoacoustic tomography (PAT) is a potential hybrid imaging modality that has attracted great attention in the fields of medical imaging. In order to generate photoacoustic signal efficiently Q-switched Nd:YAG pump lasers capable of generating tens of millijoules of nanosecond laser pulses have been widely used. However, PAT systems using such lasers have limitations in clinical applications because of their high cost, large size, and cooling requirements. Furthermore, the low pulse repetition rate (PRR) of tens of hertz is not suitable for real-time PAT. So, there is a need for inexpensive, compact, simple, fast imaging system for clinical applications. Nanosecond pulsed laser diodes could meet these requirements. In this work, we present a high-speed photoacoustic tomography imaging system that uses a compact and yet relatively powerful near-infrared pulsed laser diode. The PAT system was tested on phantoms to verify its potential imaging speed. Photoacoustic reconstructed images at different scanning speeds are presented. With single ultrasound detector scanning, the system could provide PA image ~10 times faster than the Nd:YAG laser based systems.

***Keyword*:** Photoacoustic tomography, Hybrid imaging, High-speed imaging, Pulsed diode laser.

INTRODUCTION

Photoacoustic imaging is a hybrid imaging tool which makes use of non-ionising pulsed laser radiation on the biological tissues.[1-5] It is one of the rapidly growing noninvasive, in vivo imaging technique owing to its deep penetration depth, good spatial resolution and high soft tissue contrast unlike other systems like confocal microscopy or two-photon microscopy, where the penetration depth is very low.[6, 7] It is a combination including the best features of pure ultrasound imaging and pure optical imaging. Ultrasound scattering is two to three orders of magnitude less than optical scattering on the basis of per-unit path length, making photoacoustic imaging break through the fundamental limitation of existing pure optical imaging. In photoacoustic imaging a short pulsed laser light illuminates the tissue. Due to light absorption by the intrinsic absorber in the body (e.g., blood, melanin, even water), there is a local temperature rise (in the order of milli degree). Then as a result of thermoelastic expansion pressure waves are generated in the form of ultrasound waves and come out of the tissue. Ultrasound transducers (detectors) receive the ultrasound waves [also known as photoacoustic (PA) waves] around the tissue surface. In Photoacoustic tomography (PAT) typically a single element detector receives the PA signals around the object (tissue sample) in full circle. Reconstruction techniques are used to map the initial pressure rise in the object which is in turn correlated to the absorption coefficient of the object.[8-13]

The applications of PAT are varied and include blood vessel imaging, Sentinel lymph node imaging, breast cancer detection and various others.[6, 14-18] The functional aspect of the PAT allows for the identification of the oxygenation level in the blood, and total blood volume. Both of these parameters provide various details on the angiogenesis which usually helps in the cancer detection. PAT mostly uses the blood as the contrast agent. When the contrast from the blood is not strong enough we can use other exogenous contrast agents like organic and inorganic contrast agents. There is lot of work going on in identifying new contrast agents which can provide better signal in comparison to blood and improve the imaging system some of them includes gold nanoparticles, nanospheres, nanocages, carbon naotubes etc. The major problem faced with respect to contrast agents are their biocompatibility and thus sometimes may need FDA approval before they can be used clinically. Therefore, at the clinical level we are left with very limited options of contrast agents.[19-27] Due to its high penetration depth of few centimetres and good spatial resolution we can use it to image the soft tissues in the body and obtain the structural details. The system uses only non-ionising radiation in the near infrared region thus making it more suited for the repetitive usage unlike Magnetic resonance imaging or Computed

[a] Email: manojit@ntu.edu.sg

tomography which uses harmful radiation. Also, the other imaging techniques causes lots of discomfort to the patients and requires them to stay still during the examination and may not be suitable to all patients, PAT on the other hand overcomes that issue by its small size and portability. However, it is always better to reduce any exposure to the radiation by developing a faster imaging technique would be highly beneficial in that respect as long as we are not losing the structural information.

In the near-infrared region the light penetrates much deeper in the tissue. As a result for deep tissue imaging near-infrared (NIR) wavelengths are preferred. Typically a Nd:YAG pump laser either pumps a dye laser or a OPO laser to generate pulsed NIR wavelength laser beam. So far, these types bulky lasers have been used in the PAT setup making this kind of system bulky, expensive, and slow (typical pulsed repetition rate for such lasers is 10-20 Hz).[28] Also, the bulky laser would mean that it needs a bulky cooling system and hence making its portability an issue and less favourable for clinical application.[29] There is a great need to develop a system which is compact, affordable, portable and have a high speed.[30] Also a smaller and portable system would be more beneficial from the clinical point of view, as there would be ease of handling for the physicians and the low cost is also an added advantage.

There are various geometries along which the scanning can be performed. We use the circular scanning where the transducer is rotated around the object in a circular motion recording the signals at various positions.[13] A simple delay-and-sum method for image reconstruction using a back projection algorithm is generally used as we are more focused on the structural information rather than quantitative images.[8] Though the system doesn't provide real time imaging it is the fastest method available for this type of imaging. To focus more on the quantitative image reconstructions, iterative image reconstructions or system matrix-based image reconstructions can also be used. However, in this work we will only focus on the time-domain back projection implementation. Also, time-domain back projection- based reconstruction is faster than the system matrix-based approach.

In this work, a pulsed diode laser is used to irradiate the object. A single element ultrasound detector rotates around the sample in full 360 degree to collect the PA signal and then a simple reconstruction algorithm is used to map the absorption map of the object. Hair phantom in water is used to test the performance of the imaging system. We have quantified the signal-to-noise ratio (SNR), resolution, and the imaging time.

EXPERIMENTATION AND RESULTS

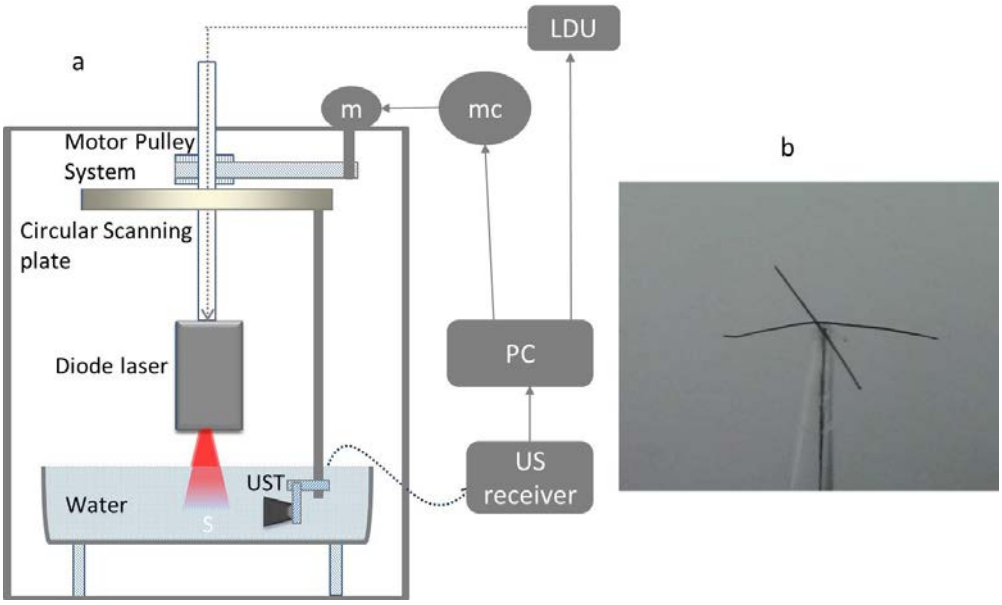

Figure 1: (a) Schematic diagram of the PAT imaging system. The sample is placed in a water bath where the laser light illuminates the sample from the top, the ultrasound transducer rotates in a full circle to record the signals from the sample. The signal is amplified, digitized, and then recorded with a data acquisition card inside a desktop PC. UST - Ultrasound Transducer, M - motor, MC - Motor Controller, LDU - Laser Directing Unit. (b) Cross hair phantom using for imaging.

Figure 1a shows the schematic diagram of the PAT system we have developed. A NIR pulsed diode laser (Quantel DQ-Q1910-SA-TEC) of ~803 nm wavelength, pulse energy ~1.45 mJ per pulse at a very high pulse repetition rate of 7 kHz illuminates the sample from the top. The laser is capable of producing ~136 nano second pulses. The sample is placed inside a water bath. We used a 5 MHz/2.25 MHz center frequency ultrasound transducer for the detection of the signal. To synchronize the acquisition of the data, same function generator (HTRONIC FG 250D) was used to trigger both the laser as well as the data acquisition system. The PA signal was first amplified with a pulse/receiver amplifier (Olympus, 5072PR) and then digitized and recorded using a data acquisition card (Gage, CompuScope 4227) connected with a desktop computer. The detector is rotated around the sample using a stepper motor (Lin Engineering, Silverpak 23C) and a homebuilt mechanical scanner. A simple MATLAB based program was used to control the data acquisition, stepper motor motion and also the reconstruction of the PA data. Figure 1b shows the phantom (a black human hair cross) used to study the imaging performance of the system. Human hair is ~50-75 micron diameter. We try different speeds of transducer rotation and try to observe the least possible time in which we can get an image with a good SNR and resolution.

For PAT typically low frequency transducers are used, as they are best suited for deep tissue imaging. Therefore in this study we used 5 and 2.25 MHz center frequency non-focused 13 mm active area diameter ultrasound detectors. Moreover, the laser pulse width is ~136 ns, which results roughly a maximum bandwidth of ~6.5 MHz of PA signals. Therefore, using a higher center frequency than this will result sub-optimal detection of the PA signals. On the other hand if we use very low frequency transducers, that will reduce the spatial resolution of the imaging system. The spatial resolution of the PAT reconstructed images is roughly related to wavelength of the detected ultrasound. For 5 MHz ultrasound the wavelength is ~300 micron. Therefore, we can achieve ~150 micron spatial resolution with 5 MHz transducer. Similarly, with 2.25 MHz detector we can achieve ~300 micron spatial resolution.

Various imaging speed was tested by controlling the transducer rotation speed. We tested 5 seconds, 10 second, 20 seconds, and 30 seconds imaging speed. Figure 2 shows reconstructed PAT images of the cross-sectional image of the phantom for various imaging speed for 2.25 MHz detector. Figure 3 shows similar images but with 5 MHz detector. All our reconstruction was done using a simple delay-and-sum back projection reconstruction algorithm in MATLAB.

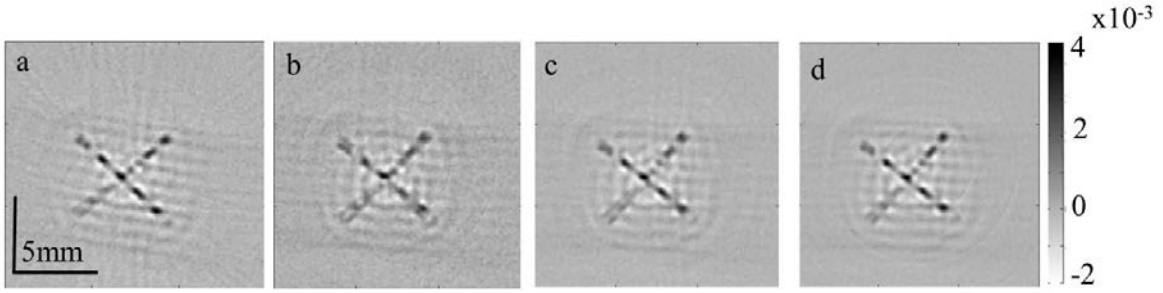

Figure 2: Reconstructed PAT images with a 2.25 MHz center frequency ultrasound transducer for various rotation speeds, (a) 5 seconds, (b) 10 seconds, (c) 20 seconds, and (d) 30 seconds.

It is evident from the Figures 2 and 3 that even with 5 s imaging speed we are able to recover the cross-sectional images with high SNR. Figure 4 shows the SNR vs scanning time. The SNR is calculated from the reconstructed image using the following formula: $SNR = \frac{A_{signal}}{\sigma_{noise}}$, where A_{signal} is the amplitude of the signal on the hair, and σ_{noise} is the standard deviation of the noise from the background. Of course with higher scan time the SNR will improve as expected. But even with 5 s scan the SNR is good enough for in vivo imaging application in the future. Moreover, even with 5 seconds rotation speed of the transducer the obtained image shows the structural features with a clarity which is not very different from the typical 30 seconds scanning speed. As expected with the higher frequency detector one can achieve high resolution imaging as seen between figure 2(a) and figure 3(a). For certain applications, the image resolution obtained with the short time scanning is just good enough and would be sufficient. The imaging was done with very fine hair structure and the images had high spatial resolution and hence we believe that we can visualise the ultrafine blood vessels in the body in a faster and cheaper.

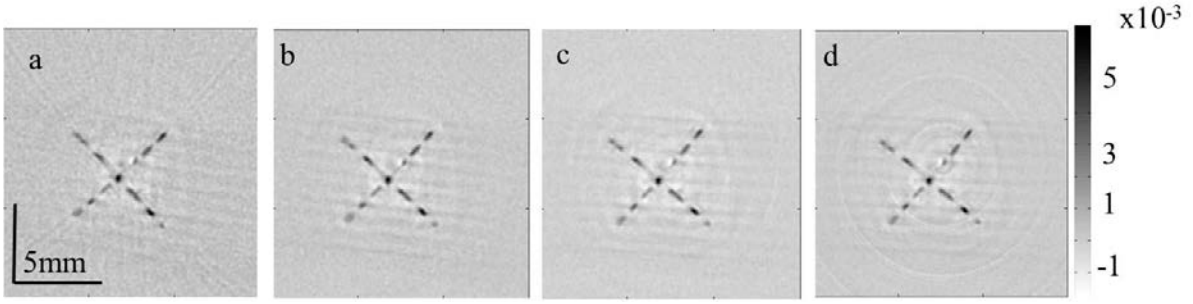

Figure 3: Reconstructed PAT images with a 5 MHz center frequency ultrasound transducer for various scanning speeds, (a) 5 seconds, (b) 10 seconds, (c) 20 seconds, and (d) 30 seconds.

Traditional lasers used for PAT has a pulse repetition rate in the order of 10-20 Hz. As a result to collect enough no of PA signals around the object the transducers need to rotate the sample slowly. As a result the image acquisition time is quite slow. Typically several minutes are needed for full rotation. However, with the use of high repetition rate pulsed diode laser we can collect data very fast (5 s) and still obtain a very good quality PAT image. This is close to 10-20 fold improvement in terms of imaging speed. From all the reconstructed images we see striated pattern in the reconstructed images. It is due to the laser beam profile. The pulse diode laser beam profile is striated and not completely homogeneous. Therefore, it is getting reflected in the reconstructed image. However, during in vivo study it will not be a problem. Since during in vivo application light has to penetrate the tissue and will get scattered. Thus the prominence of the striated pattern will reduce.

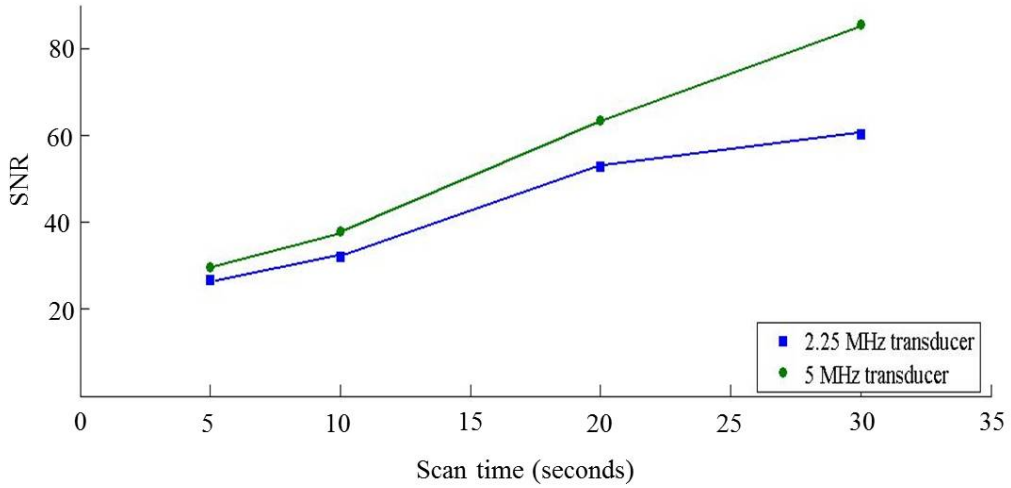

Figure 4: Signal-to-noise ratio (SNR) versus various scanning speed.

The imaging speed can further be improved by using multiple detectors. For example we can use 4-8 detectors and data can be collected in parallel. Thus another factor of 8 improvements is feasible. Thus it is possible to obtain PAT images less than one second scan-time. That way real-time PAT imaging is possible and several dynamic study can be done.

Laser Safety Limit: When PAT is used to image subjects in vivo, the maximum permissible pulse energy and the maximum permissible pulse repetition rate are governed by the ANSI laser safety standards.[31] The safety limits for the skin depend on the optical wavelength, pulse duration, exposure duration, and exposure aperture. In the spectral region of 700-1050 nm, the maximum permissible exposure (MPE) on the skin surface by any single laser pulse should not exceed $20\times10^{2(\lambda-700)/1000}$ mJ/cm^2 (where λ is the wavelength in nm). At 803 nm, for example, the MPE is 32.1 mJ/cm^2. In our imaging system, the pulsed diode laser provides ~1.4 mJ pulse energy and the laser beam spread over an area ~4 cm^2 (1.5 cm X 2.5 cm). Therefore, the laser fluence is around 0.35 mJ/cm^2. Thus, the fluence is well within the ANSI MPE. In addition, if the same area on the skin is exposed to laser light for more than 10 s, the mean irradiance should not exceed 200 mW/cm^2 in the 700–1400 nm region. However, we show that with 5 s imaging time we are able to obtain high SNR PAT images, therefore, do not require long time laser exposure.

CONCLUSION

In this work, we showed that using a high repetition rate low cost pulsed diode laser we can significantly improve the PAT imaging speed. We showed at even with 5 s scan time it is possible to obtain high SNR cross-sectional PAT images. Cross-hair phantoms were used for the imaging and with both 5 and 2.25 MHz transducers we were able to get good quality PAT images. In the future, the imaging depth capability of the system will be tested and also in vivo experiments will be done.

ACKNOWLEDGMENT

The authors would like to acknowledge Mr. Chow Wai Hoong Bobby for the machine shop support, and the financial support from the Start-up Grant by Nanyang Technological University (SUG: M408120000) and Tier 1 grant funded by the Ministry of Education in Singapore (RG31/14: M401120000).

REFERENCES

[1] Beard, P., “Biomedical photoacoustic imaging,” Interface Focus, 1, 602-31 (2011).
[2] Dean, J., Gornstein, V., Burcher, M. *et al.*, "Real-time photoacoustic data acquisition with Philips iU22 ultrasound scanner." 6856, 685622.
[3] Wang, L. V., Zhao, X., Sun, H. *et al.*, “Microwave-induced acoustic imaging of biological tissues,” Review of Scientific Instruments, 70(9), 3744-48 (1999).
[4] Wang, X., Fowlkes, J. B., Cannata, J. M. *et al.*, “Photoacoustic imaging with a commercial ultrasound system and a custom probe,” Ultrasound in Medicine & Biology, 37(3), 484-92 (2011).
[5] Pramanik, M., Ku, G., Li, C. *et al.*, “Design and evaluation of a novel breast cancer detection system combining both thermoacoustic (TA) and photoacoustic (PA) tomography,” Medical Physics, 35(6), 2218 (2008).
[6] Erpelding, T. N., Kim, C., Pramanik, M. *et al.*, “Sentinel Lymph Nodes in the Rat : Noninvasive Photoacoustic and US imaging with a clinical US system,” Radiology, 256(1), 102-110 (2010).
[7] Wang, X., Xie, X., Ku, G. *et al.*, “Noninvasive imaging of hemoglobin concentration and oxygenation in the rat brain using high-resolution photoacoustic tomography,” Journal of Biomedical Optics, 11(2), 024015 (2006).
[8] Xu, M., and Wang, L. V., “Time-domain reconstruction for thermoacoustic tomography in a spherical geometry,” IEEE Transactions on Medical Imaging, 21(7), 814-22 (2002).
[9] Xu, Y., Feng, D. Z., and Wang, L. V., “Exact frequency-domain reconstruction for thermoacoustic tomography - I: Planar geometry,” IEEE Transactions on Medical Imaging, 21(7), 823-828 (2002).
[10] Xu, Y., Xu, M. H., and Wang, L. V., “Exact frequency-domain reconstruction for thermoacoustic tomography - II: Cylindrical geometry,” IEEE Transactions on Medical Imaging, 21(7), 829-833 (2002).
[11] Shaw, C. B., Prakash, J., Pramanik, M. *et al.*, “Least squares QR-based decomposition provides an efficient way of computing optimal regularization parameter in photoacoustic tomography,” Journal of Biomedical Optics, 18(8), 080501 (2013).
[12] Prakash, J., Raju, A. S., Shaw, C. B. *et al.*, “Basis pursuit deconvolution for improving model-based reconstructed images in photoacoustic tomography,” Biomedical Optics Express, 5(5), 1363 (2014).
[13] Pramanik, M., “Improving tangential resolution with a modified delay-and-sum reconstruction algorithm in photoacoustic and thermoacoustic tomography,” Journal of the Optical Society of America A, 31(3), 621-7 (2014).
[14] Aguirre, A., Gamelin, J., Guo, P. *et al.*, "Feasibility study of three-dimensional co-registered ultrasound and photoacoustic imaging for cancer detection and visualization." 6856, 68562A.

[15] Piras, D., Steenbergen, W., van Leeuwen, T. G. *et al.*, “Photoacoustic Imaging of the Breast Using the Twente Photoacoustic Mammoscope: Present Status and Future Perspectives,” IEEE Journal of Selected Topics in Quantum Electronics, 16(4), 730-739 (2010).
[16] Ashkenazi, S., Huang, S.-W., Horvath, T. *et al.*, "Oxygen sensing for in vivo imaging by photoacoustic lifetime probing." 6856, 68560D.
[17] Cai, X., Kim, C., Pramanik, M. *et al.*, “Photoacoustic tomography of foreign bodies in soft biological tissue,” Journal of Biomedical Optics, 16(4), 046017 (2011).
[18] Pramanik, M., and Wang, L. V., “Thermoacoustic and photoacoustic sensing of temperature,” Journal of Biomedical Optics, 14(5), 054024 (2009).
[19] Kolkman, R. G. M., Steenbergen, W., and van Leeuwen, T. G., “In vivo photoacoustic imaging of blood vessels with a pulsed laser diode,” Lasers in Medical Science, 21(3), 134-9 (2006).
[20] Pan, D., Pramanik, M., Senpan, A. *et al.*, “Molecular photoacoustic imaging of angiogenesis with integrin-targeted gold nanobeacons,” FASEB J, 25(3), 875-82 (2011).
[21] Pan, D., Pramanik, M., Senpan, A. *et al.*, “Near infrared photoacoustic detection of sentinel lymph nodes with gold nanobeacons,” Biomaterials, 31(14), 4088-93 (2010).
[22] Pan, D., Pramanik, M., Senpan, A. *et al.*, “A facile synthesis of novel self-assembled gold nanorods designed for near-infrared imaging,” Journal of Nanoscience and Nanotechnology, 10(12), 8118-8123 (2010).
[23] Pan, D., Pramanik, M., Senpan, A. *et al.*, “Molecular photoacoustic tomography with colloidal nanobeacons,” Angew Chem Int Ed Engl, 48(23), 4170-3 (2009).
[24] Pan, D., Pramanik, M., Wickline, S. A. *et al.*, “Recent advances in colloidal gold nanobeacons for molecular photoacoustic imaging,” Contrast Media Mol Imaging, 6(5), 378-88 (2011).
[25] Pramanik, M., Song, K. H., Swierczewska, M. *et al.*, “In vivo carbon nanotube-enhanced non-invasive photoacoustic mapping of the sentinel lymph node,” Phys Med Biol, 54(11), 3291-301 (2009).
[26] Pramanik, M., Swierczewska, M., Green, D. *et al.*, “Single-walled carbon nanotubes as a multimodal-thermoacoustic and photoacoustic-contrast agent,” Journal of Biomedical Optics, 14(3), 034018 (2009).
[27] Kim, C., Favazza, C., and Wang, L. V., “In vivo photoacoustic tomography of chemicals: high-resolution functional and molecular optical imaging at new depths,” Chemical Reviews, 110(5), 2756-82 (2010).
[28] Daoudi, K., van den Berg, P. J., Rabot, O. *et al.*, “Handheld probe integrating laser diode and ultrasound transducer array for ultrasound/photoacoustic dual modality imaging,” Optics Express, 22(21), 26365 (2014).
[29] Daoudi, K., van den Berg, P. J., Rabot, O. *et al.*, "Handheld probe for portable high frame photoacoustic/ultrasound imaging system." 8581, 85812I.
[30] Rabasović, M. D., Nikolić, M. G., Dramićanin, M. D. *et al.*, “Low-cost, portable photoacoustic setup for solid samples,” Measurement Science and Technology, 20(9), 095902 (2009).
[31] Laser Institute of America, American National Standard for Safe Use of Lasers ANSI Z136.1-2000 (American National Standards Institute, Inc., New York, NY, 2000).